CONTRIBUTION TOWARDS A DRAFT REVISION OF RECOMMENDATION 681: PROPAGATION DATA REQUIRED FOR THE DESIGN OF EARTH-SPACE LAND MOBILE TELECOMMUNICATIONS SYSTEMS

F. Davarian and D. Bishop
Jet Propulsion Laboratory
California Institute of Technology
Pasadena, California

Abstract

Propagation models that can be used for the design of earth-space land mobile-satellite telecommunications systems are presented. These models include: empirical roadside shadowing, attenuation frequency scaling, fade and non-fade duration distribution, multipath in a mountain environment, and multipath in a roadside tree environment. Propagation data from helicopter-mobile and satellite-mobile measurements in Australia and the United States were used to develop the models.

1. Introduction

A simple method for calculating fade depth due to roadside shadowing in typical land mobile satellite environments is presented. A frequency scaling model for signal attenuation is shown. Models for fade and non-fade duration distributions are given. Also, models for clear line-of-sight degradation due to multipath are shown. The models were developed from land mobile satellite measurements.

Working Party 5B examined Recommendation 681 and Report 1009 at its meeting in 1991 in Geneva. At that time, the Working Party decided that Report 1009 did not contain sufficient prediction models to support a revision of Recommendation 681. Recent studies in the United States of America have developed additional propagation prediction models for use in the design and planning of land mobile satellite systems. The models combined with contributions from other administrations should permit the drafting of a revision of Recommendation 681 using Report 1009 as a basis.

2. Empirical Roadside Shadowing Model

Cumulative L-Band fade distributions derived from helicopter-mobile and satellite-mobile measurements in central Maryland, USA have enabled the formulation of an Empirical Roadside Shadowing (ERS) model [Goldhirsh and Vogel, 1992]. The measurements were performed on highways, where the roadside trees were primarily

of the deciduous variety. In order to assess the extent by which the trees populate the roadside, a quantity called percentage of optical shadowing (POS) was defined. This represents the percentage of optical shadowing caused by roadside trees at a path elevation angle of 45° in the direction of the signal source -- the same azimuth as the satellite or the helicopter. A model that is valid for 55% ≤ POS ≤ 75% is given as

$$A(\theta, P) = \alpha(P) + \beta(P)\theta + \gamma(P)\theta^2 \qquad (1)$$

for

$$20° \leq \theta \leq 60°$$
$$1\% \leq P \leq 20\%,$$

where A is the fade exceeded in dB, P is the percentage of the distance traveled over which the fade is exceeded, and θ is the path elevation angle to the satellite. The parameters, α(P), β(P), and γ(P) are tabulated in Table 1.

Table 1. Values α(P), β(P), and γ(P) of the ERS Model

Percentage (P)	α(P)	β(P)	γ(P)
20	24.45	-0.7351	5.991×10^{-3}
10	26.84	-0.6775	4.605×10^{-3}
5	29.22	-0.6000	3.219×10^{-3}
2	32.38	-0.5106	1.386×10^{-3}
1	34.76	-0.4430	0.0

The ERS model corresponds to an overall average driving condition encompassing right and left lane driving and opposite directions of travel along highways and rural roads where the overall aspect of the propagation path was, for the most part, orthogonal to the lines of roadside trees and utility poles. The dominant cause of LMSS signal attenuation is canopy shadowing. Figure 1 shows plots of fade exceeded versus the path elevation angle for several constant percentages.

Similar fade measurements were taken in south-eastern Australia. Left-hand circularly polarized continuous-wave transmissions from the Japanese ETS-V satellite at 1545.15 MHz were used. For the 51° elevation angle, the probability of fade exceeded in the Australian data may be described by the following best fit exponential model,

$$P(A) = u \times \exp(-v \times A) \qquad (2)$$

for

$$2 \; dB \le A \le 15 \; dB,$$

where P and A are the same as in Equation 1. The coefficients, u and v, are given in Table 2.

The "moderate" condition in Table 2 corresponds to measurements in which there was 50% to 75% optical shadowing. The "extreme" condition corresponds to measurements in which persistent shadowing occurred. The rms deviations of the measured distributions relative to the best fit curves are included. For small percentages (P = 1% to 2%) and moderate optical shadowing, the model in Equation 2 produces similar results to the model in Equation 1.

Table 2. Best Fit Exponential Cumulative Fade Distribution
Parameters for a Path Elevation Angle of 51°

Road Type	u	v	RMS Error (dB)	Fade Range (dB)
Moderate	17.57	0.2184	0.1	2-13
Extreme	95.78	0.1951	0.3	2-15

3. Attenuation Frequency Scaling Model

Mobile fade measurements [Goldhirsh and Vogel, 1992] at L-Band (1.5 GHz) and UHF (870 MHz) have shown that the ratio of fades at equal probability values is approximately consistent with the ratio of the square root of frequencies.

$$A(f_L) = A(f_{UHF}) \sqrt{\frac{f_L}{f_{UHF}}} \qquad (3)$$

for

$$1\% \le P \le 30\%,$$

where A is the fade exceeded in dB, f_L is the L-Band frequency, and f_{UHF} is the UHF

frequency.

Twenty-four sets of measurements were made driving along tree-lined roads in Central Maryland, USA. The total driving distance was 480 km. Path elevation angles of 30°, 45°, and 60° were used. For frequencies of 1.5 GHz (L-Band) and 870 MHz (UHF), using Equation 3, the predicted ratio of attenuations is 1.31. The ratio of measured attenuations had this mean and an rms deviation of ±0.1 from this value. The scaling applies in the range of P (where P is the percentage of distance traveled over which the fade is exceeded) between 1% and 30%.

An independent validation of Equation 3 is provided by a set of multifrequency measurements [Bundrock and Harvey, 1988] at 893 MHz, 1550 MHz, and 2660 MHz. The average error between these measurements and the model is less than 6%. This validation extends the applicability of Equation 3 to approximately 3 GHz.

4. Fade Duration Distribution Model

Optimal design of land mobile satellite receivers depends on knowledge of the statistics associated with fade durations. Fade duration results at L-Band were obtained from measurements in south-eastern Australia. These measurements were used to develop a model for the cumulative distribution of fade durations [Hase, Vogel, and Goldhirsh, 1991]. The south-eastern Australia measurements were taken with left-hand circularly polarized continuous-wave transmissions radiated from the Japanese ETS-V satellite at 1545.15 MHz. The in- and quadrature-phase detector voltages with noise bandwidths of 500 Hz (one-sided) were recorded at a 1 kHz rate. The output from a power detector with a predetection bandwidth of 200 Hz was recorded at a 1 kHz rate, also. The receiving antenna was of the crossed drooping dipole type with 4 dB gain, an azimuthally omni-directional radiation pattern, and a relatively flat elevation pattern over a beamwidth of 15° to 75°. Fade duration results were obtained by analyzing the average of two consecutive 1 millisecond samples. Fade durations were expressed in units of traveled distance (meters) for which the fades were continuously larger than or equal to thresholds ranging from 1 to 8 dB. Distance duration may be converted to time duration by dividing by the vehicle speed. The fade durations were observed to follow the lognormal distribution. For $dd \geq 0.02$ m:

$$P(FD > dd \mid A > A_q) = \frac{1}{2}\left(1 - erf\left[\frac{\ln(dd) - \ln(\alpha)}{\sqrt{2}\ \sigma}\right]\right), \qquad (4)$$

where $P(FD > dd \mid A > A_q)$ represents the probability that the distance fade duration, FD, exceeds the distance, dd, under the condition that the attenuation, A, exceeds A_q.

Also, σ is the standard deviation of ln(dd), and ln(α) is the mean value of ln(dd). The left-hand side of Equation 4 was estimated by computing the percentage number of "duration events" that exceed dd relative to the total number of events for which A > A_q. Figure 2 contains a plot of P versus dd (Equation 4) for a 5 dB fade threshold. The best fit regression values are α = 0.22 and σ = 1.215. Table 3 contains the RMS deviations of cumulative distributions of fade durations for various runs relative to the log-normal fit of Equation 4. Equations 2 and 4 may be multiplied to yield the joint probability that FD exceeds dd and A exceeds A_q.

Fade durations, were also derived from measurements at L-Band, taken in central Maryland, USA [Goldhirsh and Vogel, 1989]. A helicopter was used as the transmitter platform with elevation angles of 30°, 45°, and 60°. Smaller elevation angles yielded larger fade durations at fixed percentages. This is consistent with increased shadowing at lower elevation angles.

Table 3. RMS Deviations Relative to Log-Normal Fit (Equation 4) of Cumulative Distributions of Fade Durations for Various Runs Exhibiting Moderate and Extreme Shadowing.

Shadowing Level	% RMS Deviation	Distance (km)
Moderate (Run 1)	16.4	33.0
Moderate (Run 2)	18.0	8.1
Extreme	13.6	2.4

5. Non-Fade Duration Distribution Model

A "non-fade duration" event of distance duration, dd, is defined as the distance over which the fade levels are smaller than a specified fade threshold. The non-fade duration model was developed from the data set that is described in section 4. The measured data fit the following expression:

$$P(NFD > dd \mid A < A_q) = \beta (dd)^{-\gamma} \qquad (5)$$

where P(NFD > dd | A < A_q) is the percentage probability that a continuous non-fade distance, NFD, exceeds the distance, dd (meters), given that the fade is smaller than the threshold, A_q. Table 4 contains the values of β and γ for roads that exhibit "moderate" and "extreme" shadowing as defined in section 2. A 5 dB fade threshold is used. The

two "moderate" runs in the table were combined to produce a single set of fit coefficients.

Table 4. Non-Fade Duration Regression Values for a 5 dB Fade
Threshold at a Path Elevation Angle of 51°

Shadowing Level	β	γ	% RMS Deviation	Distance (km)
Moderate (Run 1)	20.54	0.58	33.3	33.0
Moderate (Run 2)	20.54	0.58	20.5	8.1
Extreme	11.71	0.8371	9.3	2.4

6. Clear Line-of-Sight Degradation Models

In many cases the mobile terminal has a clear line-of-sight to the mobile satellite. Degradation to the signal can still occur under these circumstances. This degradation may be caused by terrain that induces multipath. The mobile terminal receives a phasor summation of the direct line-of-sight signal and several multipath signals. These multipath signals may add constructively or destructively to result in signal enhancement or fade. The multipath signal characteristics depend on the scattering cross-sections of the multipath reflectors, their number, the distances to the receiving antenna, the field polarizations, and receiving antenna gain pattern.

Degradation measurements were made at L-Band and UHF. The receiving antennas were mounted on a van about 2.4 meters above the ground. The antenna patterns were omni-directional in azimuth. Between elevation angles of 15° and 75° the gain varied only 3 dB. Below the horizontal the antenna gain was reduced at least 10 dB.

6.1 Multipath in a Mountain Environment

Experiments were conducted in canyon passes in Colorado, USA [Vogel and Goldhirsh, 1988]. The transmitter was located on a helicopter that flew behind the receiver, which was located on a van. A fixed distance and path depression angle were maintained between the transmitter and receiver. L-Band (1.5 GHz) and UHF (870 MHz) signals were used. The terrain through the canyon was varied. The wall facets were variable in height, orientation, foliage overlay, and distance from the roads. Patches of trees protruded from the canyon walls. The roads contained many twists and turns.

Distributions of fade depth were determined from these experiments. The measured data was modeled with a least square power curve fit.

$$P = a \times A^{-b} \qquad (6)$$

for

$$1\% \leq P \leq 10\%$$

where P is the percentage of distance over which the fade is exceeded, and A is the fade exceeded in dB. The curve fit parameters, a and b, are shown in Table 5.

Figure 3 contains curves of the cumulative fade distributions for path elevation angles of 30° and 45° at L-Band and UHF. Four runs of 87 km total length were taken through two canyon passes (Boulder and Big Thompson Canyons). Each curve on Figure 3 is

Table 5. Parameters for Best Fit Cumulative Fade Distribution
for Multipath in Mountainous Terrain

Frequency (GHz)	Elevation = 30°		Elevation = 45°	
	a	b	a	b
0.870	34.52	1.855	31.64	2.464
1.5	33.19	1.710	39.95	2.321

derived from a subset of these four runs. The curve fits agree with the measured cumulative distribution data points to within 0.1 dB rms.

From Figure 3, the fades are 2 to 5 dB for the 45° elevation and 2 to 8 dB for the 30° elevation. The L-Band signals exhibit larger fades than the UHF signals. This could be due to tree fading, or there could have been reflecting facets on the canyon walls that were closer to the L-Band wavelength. The larger fades at 30° elevation angle can, in addition to reasons of scattering geometry, be attributed to the increased propagation path through trees and foliage.

6.2 Multipath in a Roadside Tree Environment

Experiments were conducted along tree lined roads in central Maryland, USA [Goldhirsh and Vogel, 1989]. The transmitter was located on a helicopter flying behind the receiver

carried by a vehicle. Measurement runs were repeated at 30°, 45°, and 60° elevation angles. Signals at UHF and L-Band were received. The measurements were relatively insensitive to path elevation. Therefore, the measurements were combined into a composite distribution for all three elevation angles. The measured data was modeled with an exponential curve fit,

$$P = u \times \exp(-vA) \qquad (7)$$

for

$$1\% \leq P \leq 50\%$$

where P is the percentage of distance over which the fade is exceeded and A is the fade exceeded in dB. The curve fit parameters, u and v, are shown in Table 6.

Figure 4 contains curves of the cumulative fade distributions for L-Band and UHF. The curve fits agree with the measured cumulative distribution data points to within 0.2 dB. Enhanced fading due to multipath would be expected for lower elevation angles (5° to 20°) where forward scattering from relatively smooth rolling terrain may be received from larger distances.

Table 6. Parameters for Best Exponential Fit Cumulative Fade
Distributions for Multipath for Tree-Lined Roads

Frequency (GHz)	u	v	Fade Range (dB)
0.870	125.6	1.116	1-4.5
1.5	127.7	0.8573	1-6

REFERENCES

Bundrock, A., and Harvey, R. [1988], Propagation Measurements for an Australian Land Mobile-Satellite System, Proceedings of Mobile Satellite Conference, pp. 119-124.

Goldhirsh, J. and Vogel, W.J. [1989], Mobile Satellite System Fade Statistics for Shadowing and Multipath from Roadside Trees at UHF and L-band, IEEE Transactions on Antennas and Propagation, Vol. AP-37, No. 4, pp. 489-498, April.

Goldhirsh, J., and Vogel, W.J. [1992], <u>Propagation Effects for Land Mobile Satellite Systems: Overview of Experimental and Modeling Results</u>, NASA Reference Publication 1274, February.

Hase, Y., Vogel, W. J., and Goldhirsh, J. [1991], <u>Fade-Durations Derived from Land-Mobile-Satellite Measurements in Australia</u>, *IEEE Transactions on Communications*, Vol. 39, No. 5, pp. 664-668, May.

Vogel, W.J., and Goldhirsh J. [1988], <u>Fade Measurements at L-band and UHF in Mountainous Terrain for Land Mobile Satellite Systems</u>, *IEEE Transactions on Antennas and Propagation*, Vol. AP-36, No. 1, pp. 104-113, June.
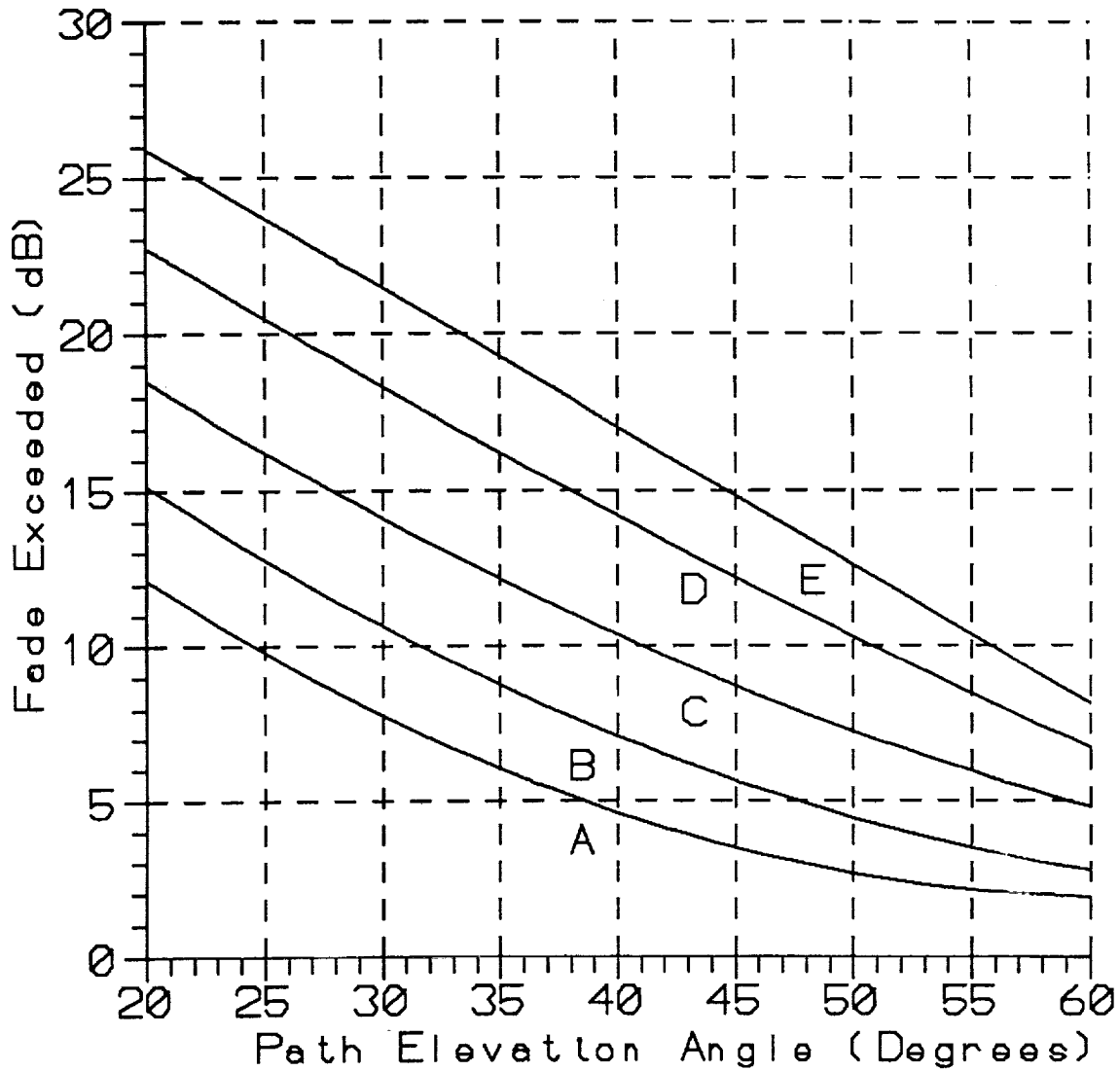
Figure 1. L-Band Fading due to Roadside Shadowing
Versus Path Elevation Angle

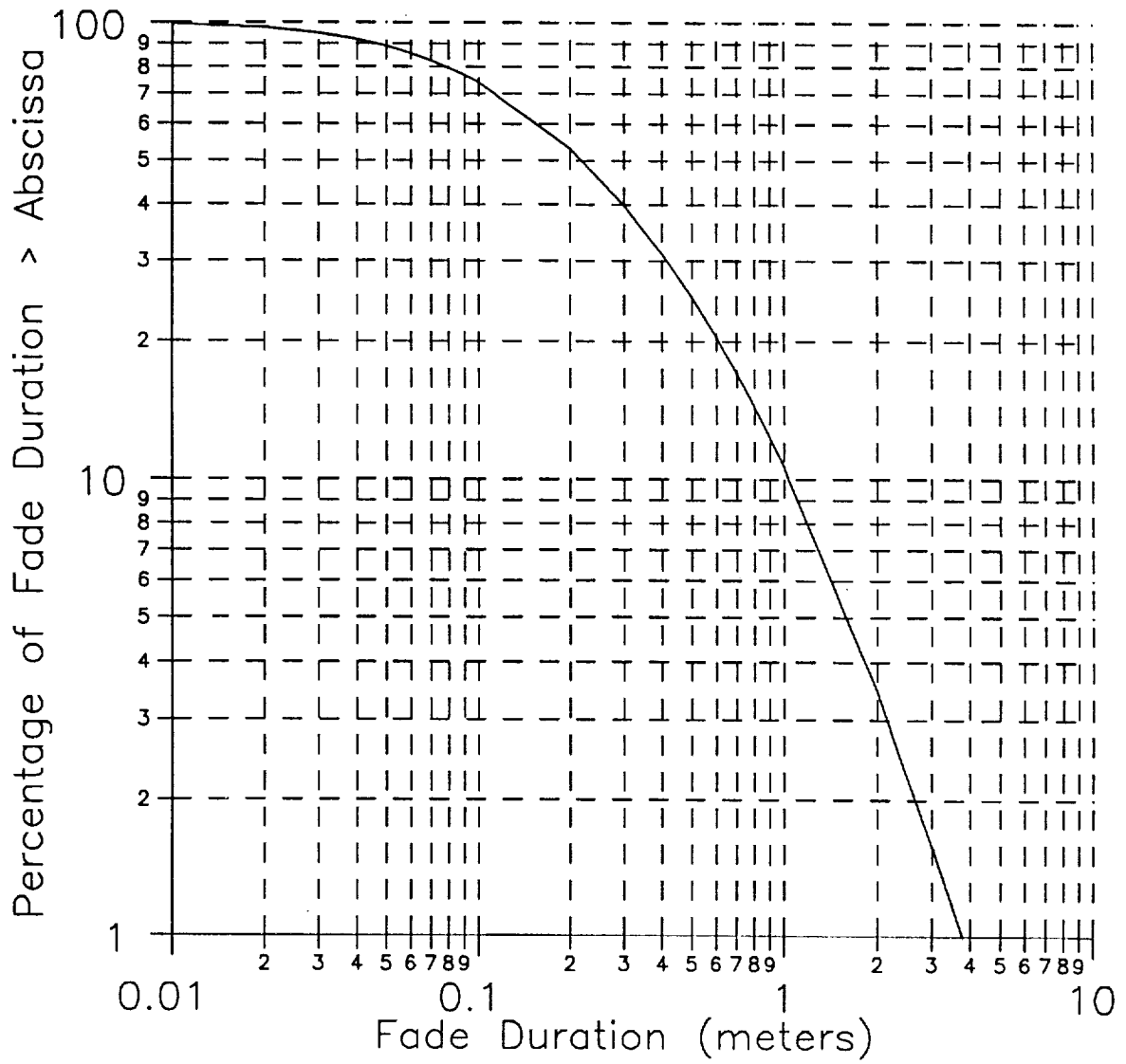A: P = 20%
B: P = 10%
C: P = 5%
D: P = 2%
E: P = 1%

Figure 2. Best Fit Cumulative Fade Distribution for Roadside Tree Shadowing with a 5 dB Threshold
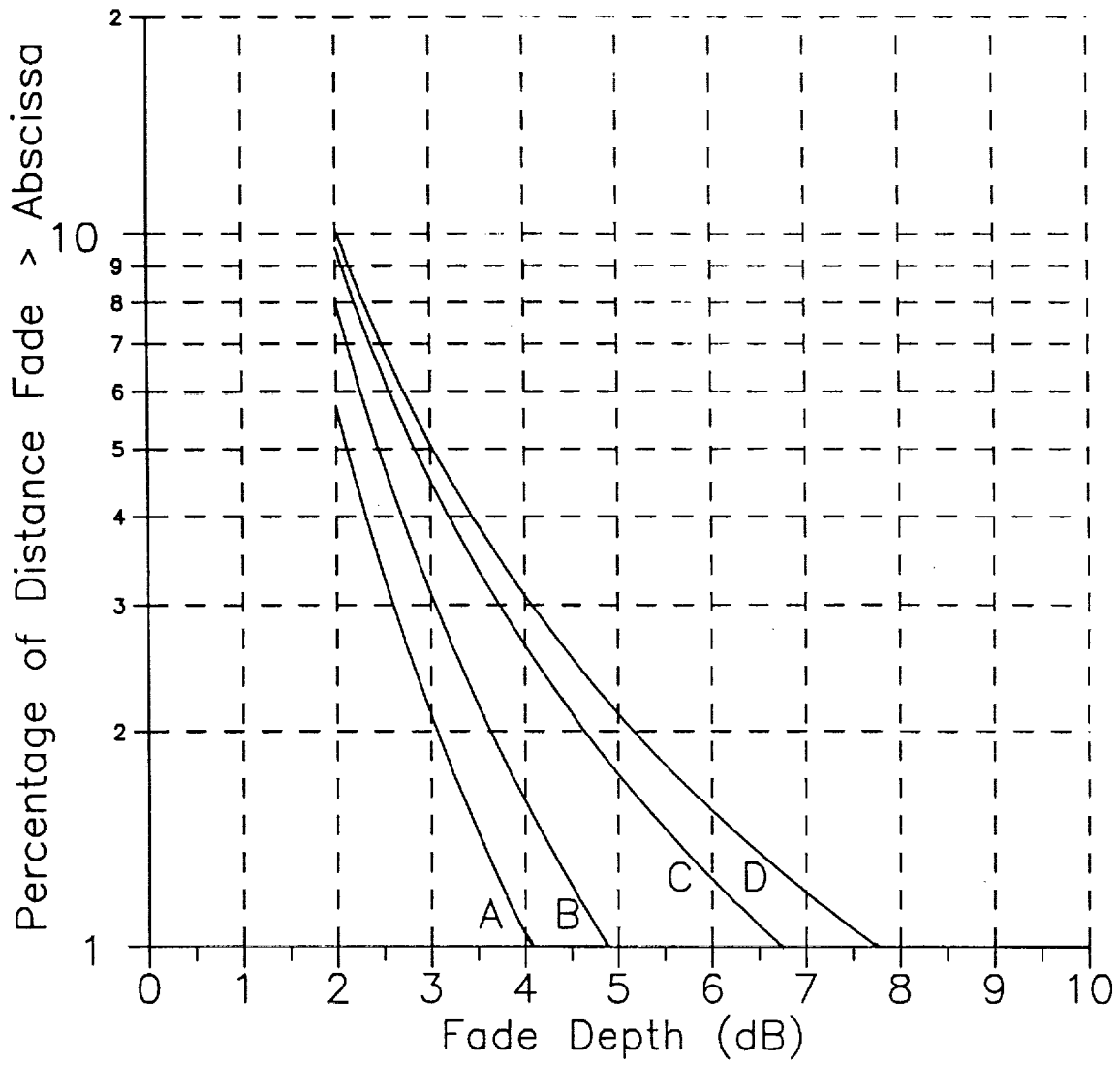
Figure 3. Best Fit Cumulative Fade Distributions for
Multipath Fading in Mountainous Terrain

A: 870 MHz, 45 Degrees
B: 1.5 GHz, 45 Degrees
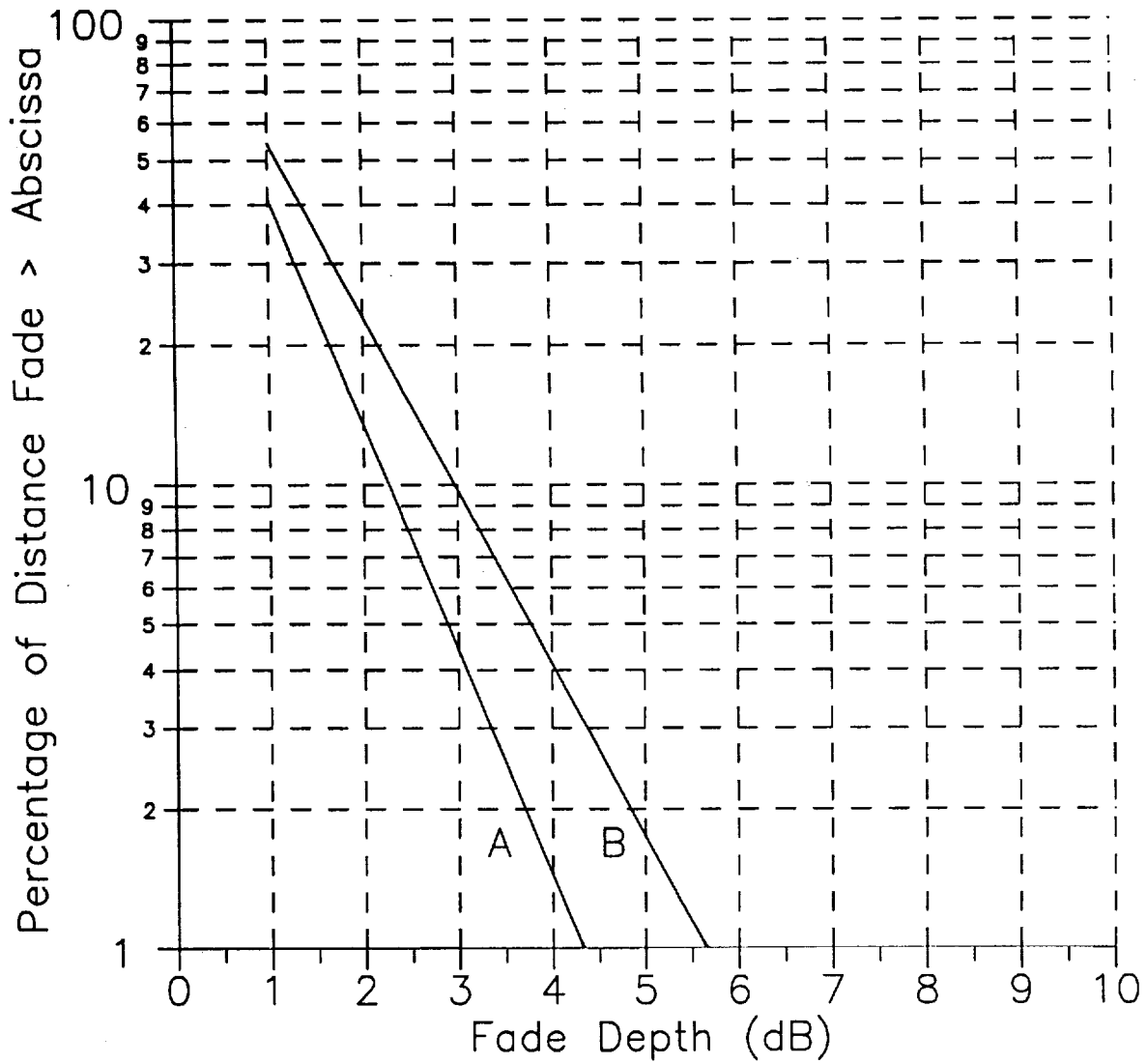C: 870 MHz, 30 Degrees
D: 1.5 GHz, 30 Degrees

Figure 4. Best Fit Cumulative Fade Distributions for Multipath Fading on Tree—Lined Roads

A: 870 MHz
B: 1.5 GHz